Modeling the roles of protein kinase Cβ and η in single-cell wound repair

William R. Holmes[a],[*],[†], Laura Liao[b],[*], William Bement[c], and Leah Edelstein-Keshet[d]
[a]Department of Mathematics and Statistics, University of Melbourne, Melbourne, VIC 3010, Australia; [b]Department of Biomedical Physics, Ryerson University, Toronto, ON M5B 2K3, Canada; [c]Department of Zoology, Laboratory of Cell and Molecular Biology, University of Wisconsin, Madison, WI 53706; [d]Department of Mathematics, University of British Columbia, Vancouver, BC V6T 1Z2, Canada

ABSTRACT Wounded cells such as *Xenopus* oocytes respond to damage by assembly and closure of an array of actin filaments and myosin-2 controlled by Rho GTPases, including Rho and Cdc42. Rho and Cdc42 are patterned around wounds in a characteristic manner, with active Rho concentrating in a ring-like zone inside a larger, ring-like zone of active Cdc42. How this patterning is achieved is unknown, but Rho and Cdc42 at wounds are subject to regulation by other proteins, including the protein kinases C. Specifically, Cdc42 and Rho activity are enhanced by PKCβ and inhibited by PKCη. We adapt a mathematical model of Simon and coworkers to probe the possible roles of these kinases. We show that PKCβ likely affects the magnitude of positive Rho–Abr feedback, whereas PKCη acts on Cdc42 inactivation. The model explains both qualitative and some overall quantitative features of PKC–Rho GTPase regulation. It also accounts for the previous, peculiar observation that ~20% of cells overexpressing PKCη display zone inversions—that is, displacement of active Rho to the outside of the active Cdc42.

INTRODUCTION

Rho, Rac, and Cdc42, belong to a family of Rho GTPases that play important roles in assembly of cytoskeletal structures in a wide variety of cellular contexts. In their active (GTP-bound) forms, these proteins associate with the plasma membrane and coordinate signals that lead to myosin phosphorylation and contraction, F-actin assembly, and, more generally, remodeling of the cytoskeleton. For example, Cdc42 and Rac activate N-WASP, which regulates assembly of branched actin filament networks via Arp2/3 (Nobes and Hall, 1995). Rho activates formins, which promote assembly of bundles of

linear actin filament arrays such as cables. Rho also activates effector proteins such as Rho kinase (ROCK), which activates myosin-2, promoting actomyosin assembly (Amano et al., 2000; Bishop and Hall, 2000). Rho-family GTPases are known to be intimately involved in orchestrating cell polarization in a variety of contexts, including single-cell motility, planar cell polarity, and neural growth cone outgrowth.

In recent years, it has become apparent that Rho GTPases are typically activated in discrete regions of the cell (termed "zones") and that this subcellular patterning is essential for their proper function (Bement et al., 2006). How this patterning occurs is poorly understood, but it likely reflects the input of GTPase-activating proteins (GAPs) and guanine nucleotide exchange factors (GEFs), which control the inactivation and activation of Rho GTPases, respectively (Moon and Zheng, 2003; Rossman et al., 2005). GAPs and GEFs are, in turn, subject to regulation by a variety of factors, including membrane lipids, reversible phosphorylation, and protein binding partners (Olofsson, 1999; Moon and Zheng, 2003; Rossman et al., 2005).

Xenopus oocyte healing offers a particularly powerful experimental model for analysis of Rho GTPase patterning. After damage, Rho and Cdc42 are rapidly activated around wounds and then segregate into concentric zones such that active Cdc42 circumscribes active Rho (Benink and Bement, 2005; see Table 1, Control image);

Conditions	Experimental observations	Image
Control	Rho zone (green) surrounds the wound, Cdc42 zone (red) beyond the Rho zone.	
PKCβ OE	Both Rho and Cdc42 zones significantly brighter. Background activity same as control.	
PKCβ DN	Both GTPase zones are suppressed. Background activity same as control.	
PKCη DN	Both GTPase zones are present, intensity same as control. Background activity for both Cdc42 and Rho increases.	
PKCη OE	In 80% of cells: loss of the Rho zone. Cdc42 zone intensity and localization relatively unchanged from controls. A faint halo of Rho is outside Cdc42 zone.	
PKCη OE "zone inversion"	In 20% of cells, both zones are present but the Rho zone is outside of the Cdc42 zone.	

TABLE 1: Summary of experimental observations for single-cell-wound GTPase patterns. Control and four experimental perturbations for PKCβ and PKCη OE and DN, from images in Vaughan *et al.* (2014), for wounds at 60 s postinjury (dark disk ~30 μm in diameter in control). This table summarizes observations used as benchmarks to distinguish among various models.

these concentric zones direct the formation of a segregated array of F-actin and myosin-2 that closes around wounds and repairs the cortical cytoskeleton (Mandato and Bement, 2001; Benink and Bement, 2005). The segregation of Rho and Cdc42 depends in part on the dual GEF-GAP Abr, which promotes local activation of Rho and local suppression of Cdc42 within the Rho zone (Vaughan *et al.*, 2011). Of importance, the Rho GTPase response to cell damage is not specific to frog oocytes: Rho is activated at the site of plasma membrane damage in yeast (Kono *et al.*, 2012), and the characteristic segregation of Rho and Cdc42 activity zones around wounds is also observed in *Drosophila* (Abreu-Blanco *et al.*, 2014) and *Xenopus* embryos (Clark *et al.*, 2009; Sonnemann and Bement, 2011).

Previous mathematical modeling showed that positive feedback between Rho and Abr along with Cdc42 autoamplification captures several basic features of the activation and segregation of Rho and Cdc42 at wound sites (Simon et al., 2013). More recently, we discovered the participation of additional players: the lipid diacylglycerol (DAG), which is rapidly generated at wound borders and is required for proper activation of Rho and Cdc42 around wounds, and two DAG targets—protein kinase C η (PKCη) and PKCβ (Vaughan, 2014). PKCη and PKCβ are rapidly recruited to wounds and form a characteristic pattern, with PKCβ overlapping both Rho and Cdc42 zones and PKCη being confined to a much narrower region near the wound edge. Although DAG stimulates both PKCη and PKCβ, these two kinases play apparently antagonistic roles in the healing process: PKCβ activates Rho and Cdc42, whereas PKCη inhibits them.

Here we sought to adapt the model originally developed for Abr, Rho, and Cdc42 dynamics in cell repair (Simon et al., 2013) to explain the potential roles of PKCη and PKCβ in Rho and Cdc42
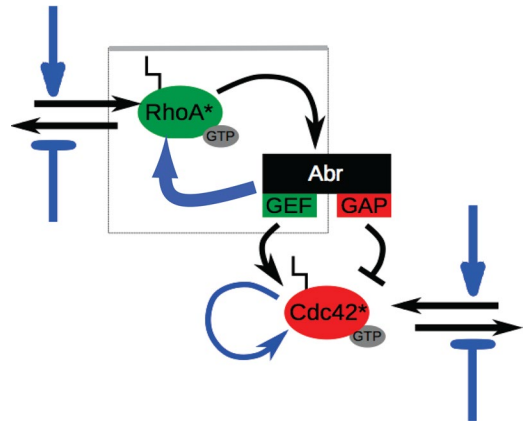

FIGURE 1: Schematic diagram showing the Rho-Abr-Cdc42 cross-talk as modeled in Simon *et al.* (2013). Here we consider the possible effects of PKCs (blue arrows) on either the basal activation rates of RhoA and Cdc42 or the magnitude of positive feedback from Cdc42 to itself and from Rho via Abr to itself.

zone formation (Figure 1). To do so, we exploited a number of observations, including how various perturbations influence Rho and Cdc42 zones qualitatively and somewhat quantitatively (extent of depression or enhancement of zone intensities). We also exploit a bizarre but intriguing observation: PKCη overexpression reduces or eliminates the Rho zone in ~80% of cells, but in the remaining ~20%, it causes "zone inversion"—displacement of the Rho zone outside the Cdc42 zone (Vaughan *et al.*, 2014). Together these diverse observations, particularly the zone inversion, provide powerful and specific "screens" with which to challenge a series of models and determine the likely targets and influence of the PKCs.

RESULTS

Model background and description

In response to a wound, Rho and Cdc42 "zones"—regions of high GTPase activity next to the wound—are observed experimentally along with background activity levels further away. It is well known in the modeling literature (Ferrell and Xiong, 2001; Tyson *et al.*, 2003) that coexistence of two distinct levels of activity generally imply bistability (i.e., multiple stable steady states) in the system. In the present case, this resides in the underlying signaling network. It could arise from cooperativity or another form of positive feedback. The core element of the bistability hypothesis is that feedback introduces a threshold separating two states. If the system is initially below that threshold, it remains in a state of low activation. If, however, a stimulus drives the system above that threshold, feedback amplification generates an even stronger activation, propelling the system to a higher state. In the context of the single-cell wound, this hypothesis was detailed in Simon et al. (2013) and shown to be consistent with experimental observations. To summarize, the essential idea is that an uninjured *Xenopus* oocyte is in the state of low GTPase activity (throughout its plasma membrane), and injury produces a stimulus that locally drives levels above a required threshold, triggering a positive feedback on the GTPase activation, thus setting up the zones of high Cdc42/Rho activity. The GTPase activity inside the zones then represents the higher of the two bistable steady states.

In this model, RhoA, Cdc42, and Abr are described by a set of reaction-diffusion equations that track the distributions of their activities over time. On the basis of the circular symmetry of the wounds, we can simplify the geometry. Here we use a one-dimensional spatial domain (distance away from the wound edge; Figure 2a) and track
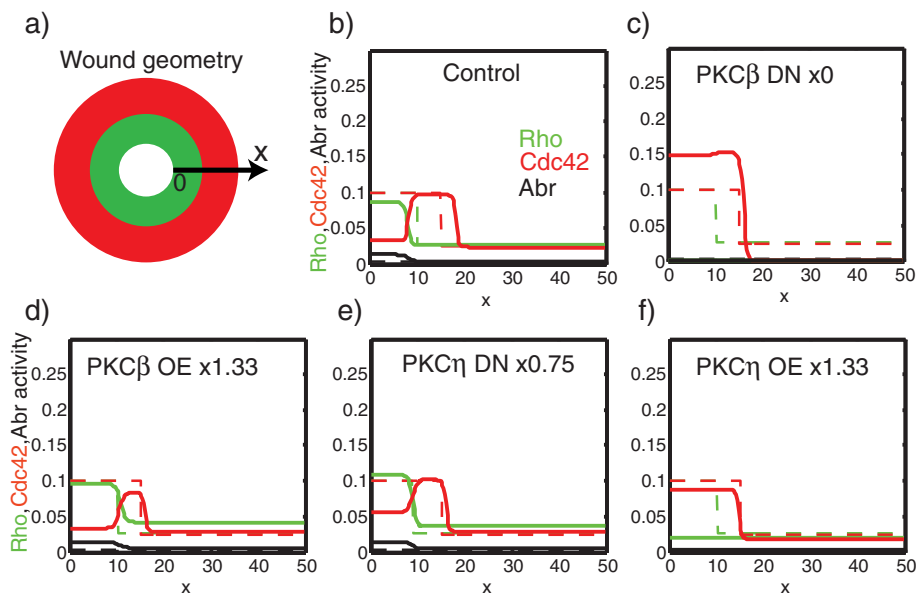
FIGURE 2: Model geometry, control simulation, and failure of the simplest model. (a) Geometry of the wound, showing the Rho and Cdc42 zones (green and red, here and throughout all figures) and our one-dimensional model (x is distance from the wound edge). (b) A control simulation showing the distributions of Rho, Cdc42, and Abr for a "wild-type" model cell, with parameter values in Supplemental Table S1. Initial conditions are shown as dashed lines, final profiles 20 s later are shown as solid lines. (c–f) Model results conflict with experimental observations when we assume that PKCs affect only the basal activation or inactivation rates of Rho and Cdc42. (c) PKCβ DN (full suppression of basal activation rates b_R, b_C) fails to extinguish the Cdc42 zone. (d) PKCβ OE (b_R, b_C increased by a factor of 1.33) hardly changes the zone intensities, failing to make them significantly brighter. (e–f) PKCη is assumed to influence basal inactivation rates (d_R and d_C) by the indicated fold change. (e) PKCη DN (no major disagreement). (f) PKCη OE suppresses Rho but allows Cdc42 to invade the region next to the wound edge, contrary to what is observed experimentally. In all cases, simulations are run for 20 s to determine how zones localize before wound closure.

the GTPase and Abr distributions on the membrane in space and time. After some simplification (Maree *et al.*, 2006; Holmes *et al.*, 2012; Lin *et al.*, 2012), each GTPase can be represented as being in one of two states—an active, membrane-bound form, and a sequestered, inactive, cytosolic form. Cycling between these two states is mediated by GEFs and GAPs, which activate and inactivate a given GTPase, respectively. We simplified the details of membrane association and disassociation. (GEFs, GAPs, and GDIs are not explicitly modeled as time-dependent variables.) This is a well-established simplification, retaining the core elements of GTPase function that are responsible for patterning responses (Maree *et al.*, 2006; Holmes *et al.*, 2012). The model thus focuses primarily on the activation and inactivation dynamics of Cdc42 and RhoA, and we investigate how PKCη and PKCβ influence those dynamics.

Much of the modeling of GTPase dynamics has focused on cell polarization. In that context, depletion of a pool of inactive GTPases was needed for robust polarization by a "wave pinning" process (Jilkine *et al.*, 2007; Mori *et al.*, 2011; Lin *et al.*, 2012; Edelstein-Keshet *et al.*, 2013; Holmes, 2014; Holmes *et al.*, 2015). Depletion stabilizes the boundar(ies) of GTPase activity and guarantees that a stable spatial pattern can be established. Here, however, the wound is small (~20–50 μm) compared with the size of a *Xenopus* oocyte (~1000 μm), so depletion has a relatively minor effect. Hence we assume that there is a constant pool of inactive GTPase available for cycling onto the membrane (activation). We therefore track only the dynamics of the membrane-bound form of each GTPase. Furthermore, rather than focusing on long-term dynamics (or steady states)

of the system, we are concerned with transient properties of the system, since the wound response occurs over a few tens of seconds and results in continual reorganization of the geometry and size of the wound. Thus in what follows we consider GTPase zone localization as transient spatially, whereas the level of GTPase activity inside and away from those zones will be associated with steady states of the regulatory kinetics.

In the original investigation of this wound-healing process, GTPase activity was further linked to downstream wound contraction. Thus wound closure and the associated advective flow of regulators were included in the model. Here we focus on the initial formation of these zones, with particular interest in their relative intensities and positions under various conditions. We thus do not model the closure process itself or the advective flows associated with it. For this reason, we use a fixed spatial domain that does not vary in time for simplicity.

Figure 1 summarizes the Rho GTPase cross-talk captured by the model equations (details are given in the Supplemental Material). Active RhoA binds Abr, which acts as a RhoGEF, setting up positive Rho feedback. This complex then acts as a GEF/GAP for Cdc42, with a dominant GAP effect at high concentrations. To generate a persistent Cdc42 zone, we showed that it was essential that Cdc42 exhibit cooperativity and autoamplification, introducing an additional Abr-independent positive feedback (Simon *et al.*, 2013). We also showed that zones become established when Rho-Abr positive feedback is triggered, driving an initial superthreshold GTPase level to the higher of two states in the spatially bistable system. Both the original model and the one discussed here represent only the time span of ~54–84 s after wounding, when other processes have set up initial Rho and Cdc42 activities. (Calcium influx and other proximal signals occur before this time.) The initial GTPase activity profile after wounding is assumed to be above threshold for Rho and Cdc42 near the wound so as to excite zone formation. We used parameter values explained previously (Liao, 2013; Simon *et al.*, 2013; Supplemental Table S1).

We previously took advantage of the fact that the model can be decomposed into two submodels to aid in analysis (Simon *et al.*, 2013). From the model schematic in Figure 1, it is apparent that Cdc42 does not influence Rho or Abr. Thus, for the purpose of analysis, it is possible to decompose the system into a Rho–Abr subsystem whose output affects the Cdc42 subsystem. This situation remains unchanged when we include the effect of PKCs. Hence we will exploit this idea in our analysis of the revised model.

Here we build on the previous basic model for Cdc42 (C), RhoA (R), Abr (A) dynamics to investigate the influence of PKCs in shaping responses. In Figure 1, blue arrows show potential PKC targets: 1) GEF-mediated basal activation rates (vertical blue arrows, model parameters b_R, b_C), 2) GEF/GDI-mediated inactivation rates (vertical blue inhibitory arrows, parameters d_R, d_C), and 3) the strength of positive feedbacks (curved blue arrows and parameters γ_{AR}, γ_C). The

subscript β or η indicates that the given parameter is influenced by PKCβ or PKCη in the model (e.g., $d\eta_R$ describes the influence of PKCη on Rho inactivation). We use standard kinetic terms to represent the rates of these biochemical processes. Positive feedback terms are taken to be Hill functions. For example, the rate of Abr-mediated RhoA activation is a function of Abr activity (A), here taken to be $\gamma_{AR}A^n/(K^n_R + A^n)$, where K^n_R is a constant. Such nonlinear terms are commonly used to account for saturating switch-like kinetics (with $n > 1$) of signaling components. We found that the Hill coefficient $n = 6$ provides the best agreement with data, although either higher or lower values will yield qualitatively similar results.

When considering PKC dynamics, we first assume that PKCβ and PKCη are spatially homogeneous for simplicity. We use results of molecular perturbation experiments as benchmark data to constrain the possible targets of PKCs and determine how they participate in the wound response. Table 1 summarizes these benchmark observations. We ask whether variations in one or another of the key model parameters can account for the observed effects of PKC overexpression (OE) and dominant-negative (DN) experiments. More specifically, we use phase plane analysis along with bifurcation diagrams to visualize how variations in model parameters affect responses. We consider both the background activity levels (characterizing GTPases outside the zones) and the GTPase zone intensities. Rather than simply validating that model against purely qualitative experimental observations (e.g., PKCβ OE increases zone intensity), we also consider some quantitative aspects of the observations (e.g., zone intensity increases markedly rather than mildly). This provides finer-grained benchmarks that will allow us to distinguish between seemingly similar possibilities.

Benchmark observations

Building on this model, we will consider the influence of PKCs on the transient zone dynamics. Both imaging and fluorescence quantification (Vaughan *et al.*, 2011) clearly indicate that PKCβ and PKCη have an important role in modulating the GTPase wound response. What remains unclear is how they modulate that response. To gain further insights into their role, we tested different hypotheses against several observations (summarized in Table 1). 1) When PKCβ is overexpressed, both Cdc42 and Rho zones are substantially brighter (implying greater levels of GTPase activity in the zones). 2) For DN PKCβ, both zones are suppressed (implying lower levels of GTPase activity). 3) For DN PKCη, both zones are relatively unaffected. 4) When PKCη is overexpressed, 80% of cells show a loss of the Rho zone, but the Cdc42 zone remains. In these cases, even though the Rho zone is lost, the Cdc42 zone is found in the same place as in the control cells and does not move closer to the wound edge. 5) In the remaining 20% of cases, both zones persist, but their spatial location is inverted, with the Cdc42 zone next to the wound and the Rho zone on the outside. This puzzling observation provides a specific criterion that we used to challenge a sequence of models. Few of the possible hypotheses met this challenge, as described later.

The foregoing experimental observations are consistent with the claim that PKCη deactivates whereas PKCβ activates the GTPases. However, how they do so, what processes they are influencing, and how they are shaping the response is not immediately apparent. In the following, we will challenge a sequence of models against these observations to test several hypotheses and suggest a mechanism of PKC action that is consistent with these data.

Rejecting the simplest model

We first considered the simplest possibility, that PKCβ enhances basal GEF activity, whereas PKCη amplifies basal GAP activity. We tested variants of this idea for spatially uniform, as well as spatially localized, PKC distributions—whether correlated with the GTPase zones or obtained directly from experimental data (Liao, 2013). This agreed with certain aspects of experimental observations. For example, we found enhancement or suppression of GTPase zones by PKCβ OE or DN, respectively, and suppression or enhancement of GTPase zones by PKCη OE or DN, respectively. However, the results failed to match quantitative aspects of the data and failed to account for zone inversion (Liao, 2013). Figure 2 demonstrates a subset of these failed attempts. We first show the wound geometry (Figure 2a) and then predictions obtained by simulating the partial differential equations of the model (see the Supplemental Material) with default parameter values (control; Table 1) and parameter variations (Figure 2, c–f). The predicted spatial distributions of Rho (green), Cdc42 (red), and Abr (black) for the wild type (control, Figure 2b) and for OE and DN of each of the PKCs (Figure 2, c–f) are displayed as functions of space at time $t = 50$ s postwounding. Fold changes in the basal Rho and Cdc42 activation rates are indicated.

For example, in Figure 2c, both basal activation rates were set to zero ($\times 0$) to mimic complete suppression (strongest possible DN effect) of the basal GEF effect on both Rho and Cdc42. Nonetheless, the Cdc42 zone still forms (due to the strength of the Cdc42 positive feedback). This conflicts with the experimental observation that for PKCβ DN, both zones are suppressed. In Figure 2d, the basal activation rates (b_R, b_C) are increased by a factor of 1.33, which would depict a PKCβ OE case. However, model predictions fail to produce zones that are any brighter than the control, in conflict with experimental observations. For the PKCη DN in Figure 2e, inactivation rates (d_R, d_C) are reduced, and the disagreement is less noticeable. For PKCη OE (Figure 2f, inactivation rates increased), the Rho zone is suppressed, and the Cdc42 remains. However, these results predict that the Cdc42 zone will invade closer to the wound edge, which is contrary to the observation that the Cdc42 zone remains in place and does not move closer to the wound edge. Thus the simple default model fails to match experimental observations and must be rejected.

Role of PKCβ in wound response

Because the simplest model, in which PKCs act on only basal GEF or GAP activities, did not suffice to explain the data, we next considered a number of variations that could plausibly correct the model deficiencies. Experimental perturbations clearly indicate that PKCβ acts to promote GTPase activity. To gain a more detailed understanding of how PKCβ shapes the wound response, we considered several activation pathways it might influence. As a first assumption, we take PKCβ to be uniformly active in the region near the wound. Next we consider different assumptions for how PKCβ might influence Rho and Cdc42 individually. For each of these GTPases, there are two primary sources of activation: basal activation (represented by the rates b_R and b_C, respectively) and feedbacks necessary for zone formation. Feedback strengths are modulated by the parameters γ_{AR} and γ_C, respectively.

To better understand the failures of the first model, we first contrast the effects of varying the simple basal activation rate (b_R) versus varying the activation strength due to the positive feedback (γ_{AR}). To do so, we consider the Rho–Abr subsystem (recall that this subsystem receives no direct inputs from Cdc42 in the model, so we can study it on its own). On the Rho–Abr plane (Figure 3, a and c) we show curves representing $dR/dt = 0$ (Rho nullclines) in green for several values of γ_{AR} (Figure 3a) and similarly for several values of b_R (Figure 3c). Also shown on the same plots is the Abr nullcline ($dA/dt = 0$, black curve). Note the intersections of (one of the) green and
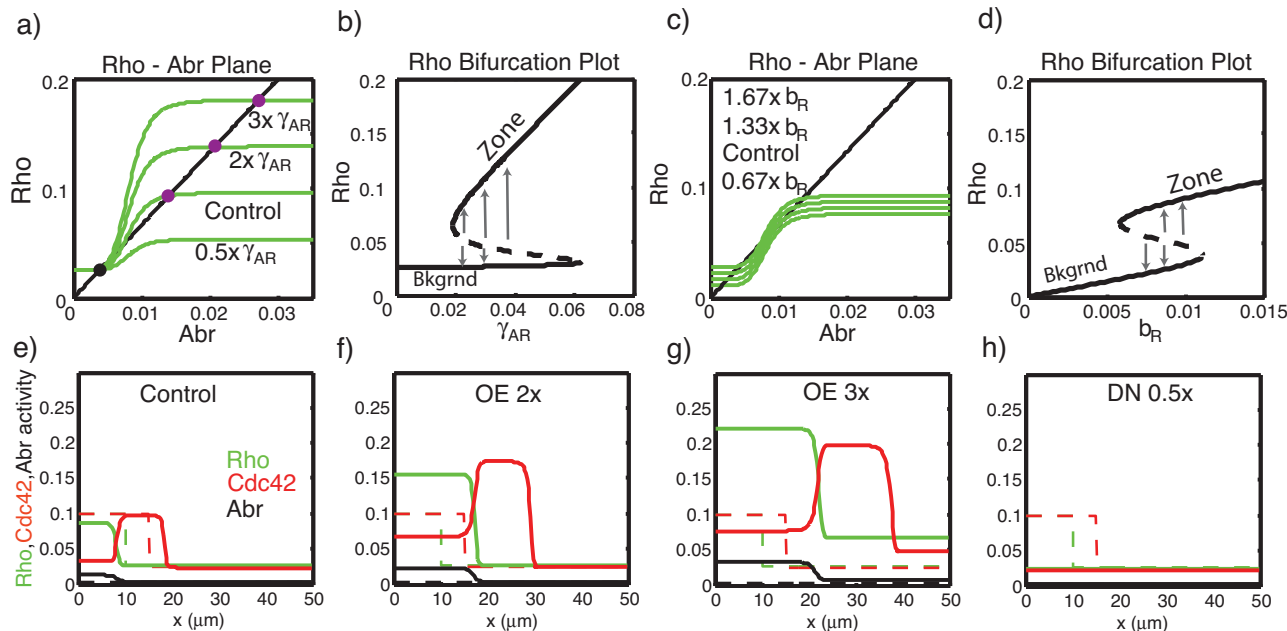
FIGURE 3: (a) Reduced Rho–Abr phase plane showing the Abr nullcline (black) and sample Rho nullclines (control as well as DN, OE2, and OE3) for multiple values of γ_{AR} (0.5, 1, 2, and threefold multiples of the value stated in Supplemental Table S1; all other parameters are as in that table). Intersections (shown in purple) are steady-state Rho intensity levels in the Rho zone, adjacent to the wound, and the black dot is background Rho activity level. (b) Bifurcation diagram showing steady-state Rho activity levels as a function of the Rho–Abr positive feedback strength γ_{AR}. The lower solid line represents the background Rho level; the upper branch represents the Rho zone intensity. Note that the two steady states can coexist over a range of the parameter values and that the intensity of the zone (but not of the background) increases sharply as the positive feedback strength γ_{AR} increases. (c) As in a, but for several values of the basal activation rate (b_R). (d) As in b, but for the parameter b_R. Note that both background and Rho-zone intensities increase with b_R but that the zone intensity increases less strongly than in b. (e) Simulation of the model "control" (wild-type cells) using parameters in Supplemental Table S1. (Initial conditions, dashed lines; final profiles, solid lines.) (f) Similar to e, but with both feedback strengths γ_{AR} and γ_C multiplied by a factor of 2 to mimic PKCβ OE (equivalent to 2× in a). Note that zones get significantly "brighter." (g) Similar to f, but with a threefold increase in the feedback strengths. (h) Similar to e–g, but with a factor of 0.5 reduction in feedback strengths to mimic PKCβ DN. Here all zones are abolished.

the black nullclines. These represent possible steady states of the Rho–Abr subsystem; the black dot represents a state with low Rho and low Abr activities (typical background levels away from the wound); the purple dot represents a state with high Rho and Abr activities (as occur within the "Rho zone"). An intermediate intersection depicts a threshold (unstable steady state) that separates these two coexisting stable steady states. The sigmoidal shape of the green curves stems from positive feedback: for low Abr, the feedback is very weak, whereas for high Abr, the feedback is strong, leading to higher Rho levels.

From Figure 3a we see that changing the feedback strength parameter γ_{AR} by some fold-multiple significantly affects the "Rho zone intensity" (moving the higher steady-state, purple dot to larger values of both Rho and Abr) while leaving the background levels of Rho and Abr (black dot) essentially unchanged. This is shown by the green curves labeled 2× and 3×, which represent possible PKC OE levels. The 0.5-fold reduction in γ_{AR}, representing a PKC DN effect, has the opposite effect, completely removing the purple intersection and thus making zone formation impossible. Again, background levels of activity remain unchanged Thus, modulating this feedback strength can either decrease the height of the purple dot relative to the control "wild type" or destroy that intersection (and hence the zone) entirely.

Contrast this with Figure 3c, which shows the effect of changes in the basal Rho activation rate, b_R. Here either increasing or

decreasing this parameter leads to changes in *both* high and low points of intersection, although by small amounts. The interpretation is that if PKC OE/DN were to affect this parameter (a hypothesis of the model we rejected), we would see changes in *both* the background Rho activity level and the Rho zone intensity but by relatively small amounts. Taken together, these results show that the magnitude of the change in Rho zone intensity is markedly larger if PKCβ is assumed to influence Rho–Abr feedback strength rather than rates of Rho basal activation.

A second way to visualize such results is with a "bifurcation diagram," which shows how the values of steady states depend on a parameter of interest. Figure 2b (respectively Figure 2d) shows the steady-state Rho activities that can be achieved as the parameter γ_{AR} (respectively b_R) increases continuously over some range of values. The lower "branch" of these z-shaped diagrams corresponds to the background Rho activity level, whereas the upper branch depicts the Rho zone intensity. An intermediate steady state (dashed portion of curve) acts as a threshold separating the two stable steady states. Arrows show typical dynamics for Rho states that start above or below that threshold. In both Figure 3, b and d, there is a range of the given parameter that corresponds to coexistence of two stable steady states ("bistability"). For example, this occurs for $0.02 \leq \gamma_{AR} \leq 0.06$ in Figure 3b.

As before, we find that the magnitude of the high steady-state activity level increases dramatically with feedback strength γ_{AR},

whereas the background level is virtually unchanged (Figure 3b). In contrast, in Figure 3d, we see that the high steady-state activity level increases only slightly, as does the background level, when the basal rate of Rho activation, b_R, is increased. A similar analysis of the Cdc42 subsystem (not shown) with respect to the basal activation and feedback strength parameters for Cdc42 (b_C and γ_C) leads to parallel conclusions.

A more detailed review of fluorescence quantification results in Vaughan *et al.* (2014) indicates that PKCβ is more likely to target feedback than basal activation. Although both possibilities capture the general trend of observations (e.g., DN conditions lead to zone suppression), a finer-grained analysis distinguishes between the two. In PKCβ OE, the fluorescence intensity for both Cdc42 and Rho is observed experimentally to increase dramatically. Moreover, for PKCβ DN, the background GTPase activity levels remain essentially unchanged. These results are consistent with effects we observe when we modulate the feedback strength parameter γ_{AR} rather than the basal activation rate b_R.

On the basis of these findings, we next asked whether perturbations of Rho/Cdc42 feedback pathways would match the spatial patterns observed experimentally in PKCβ OE and DN conditions (Vaughan *et al.*, 2014). Accordingly, we again simulated the full system of partial differential equations of the model with default parameter values (Supplemental Table S1) and specific parameter variations. For ease of comparison, we show the control in Figure 3e. Figure 3, f–h, demonstrates results for two levels of OE (2×, 3× fold changes) and one DN value (0.5× fold change) of the feedback strength parameters γ_{AR} and γ_C. We find that strengthening both

Cdc42 and Rho–Abr feedbacks leads to a dramatic increase (greater than twofold) in GTPase activity levels (within the zone), whereas the simulated DN condition leads to complete suppression of the zones. Taken together, these results suggest that the feedback processes responsible for zone generation in this system are a likely target of PKCβ activity.

Role of PKCη in wound response

We next sought to characterize the role of PKCη in the wound response. As noted, PKCη OE attenuates Rho and Cdc42 activities in experimental observations. In PKCη DN experiments, fluorescence quantification shows that whereas background GTPase activity levels appear to increase, zone brightness does not significantly increase. We asked what model parameters could account for such observations.

We considered two possibilities for the underlying mechanism. One possibility is that PKCβ and PKCη both influence the same GTPase positive feedback but with opposing effects. In that case, arguments detailed in the preceding section can be adapted to analyze PKCη's role. A second possibility is that PKCη acts through a distinct pathway, for example, enhancing a GAP or related pathway to inactivate the GTPases or damping a GEF pathway to inhibit GTPase activation.

We consider these possibilities individually. Based on the foregoing findings, it is unlikely that PKCη influences feedback strength: we already noted that a reduction in feedback strength would lead to a dramatic reduction in zone brightness (Figure 3, a and b), in disagreement with PKCη DN experimental results (increasing background, but no major increase in zone brightness). Hence we reject this possibility. This leaves two possibilities: PKCη either increases GTPase inactivation or suppresses GTPase basal activation. Although subtle differences between these possibilities exist in model predictions, the data fail to distinguish between the two scenarios. Hence we select one to explore.

Suppose that PKCη acts directly on GTPase inactivation (through the parameters $d\eta_R$ and $d\eta_C$). For simplicity, let us first assume that PKCη is spatially uniform near the wound. We now consider the Cdc42 model subsystem. This corresponds to a single differential equation (as distinct from the two-variable Rho–Abr subsystem that we represented on a Rho–Abr plane). However, we can still observe the effect of parameters on Cdc42 steady-state values in a geometric way by plotting Cdc42 rate of activation (red curve) and rates of inactivation (black curves, for various values of $d\eta_C$) together on the same diagram (Figure 4a). (Positive feedback of Cdc42 generates the sigmoidal shapes of the red curves.) Then points of intersection of a red and a black curve (where activation and inactivation rates balance) correspond to Cdc42 activity levels for which the net activation rate is zero ($dC/dt = 0$). The Cdc42 values of these points (horizontal axis) are precisely the steady-state Cdc42 levels. We mark the low steady states (background Cdc42 activity
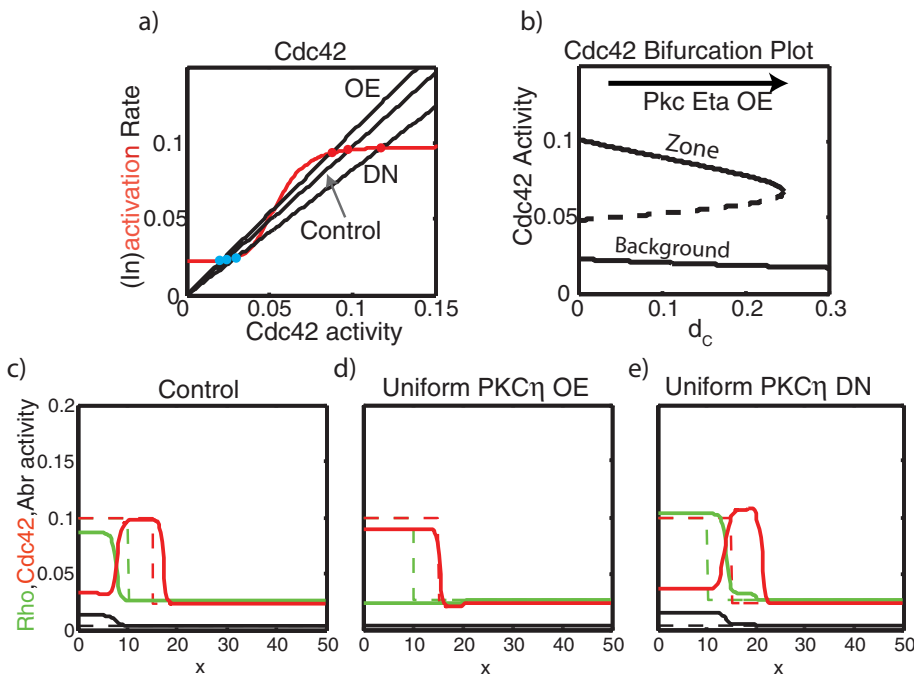

FIGURE 4: (a) Diagram showing the Cdc42 rates of activation (red curve) and three sample inactivation (black) rates vs. Cdc42 activity levels. The three black lines correspond to PKCη OE, WT, and DN ($d\eta_C = -0.15, 0, 0.1$, respectively). Intersections of red and black curves are Cdc42 steady-state levels, with red dots representing the elevated Cdc42 intensities in the Cdc42 zone and the blue dots (practically all the same) indicating background Cdc42 activity levels. All other parameters are as in Supplemental Table S1. (b) Cdc42 bifurcation plot with respect to the strength of PKCη-mediated Cdc42 inactivation. (c) Control (WT) simulation for comparison purposes. (d) Spatial behavior. Formation of a single Cdc42 zone for spatially uniform PKCη OE ($d\eta_C$ and $d\eta_R = 0.1$ with η = 1 uniformly on the domain.) (e) Simulation of reduced inactivation for PKCη DN: the parameters $d\eta_C$ and $d\eta_R$ are reduced, but zone intensity hardly changes.

levels) with blue dots and the Cdc42 zone activity level with red dots for three possible PKCη conditions: control, DN, and OE. As seen in Figure 4a, PKCη DN (OE) increases (decreases) the Cdc42 activity levels, but the change is relatively small, on the order of 10% of control.

We summarize the effect of PKCη in the bifurcation diagram of Figure 4b. Here the vertical axis represents the steady-state Cdc42 activity level, and the horizontal axis is the level of PKCη represented by variation of the parameter d_C. Low and high steady states coexist for much of the displayed range of PKCη, consistent with the presence of distinct background versus zone Cdc42 activity levels ("bistability"). The intensity of the Cdc42 zone steady state depends only weakly on PKCη activity level: both upper and lower branches of the z-shaped curve have a shallow slope.

We next simulated the full model to visualize the spatial distribution of Rho, Cdc42, and Abr, as before, with the control simulation repeated in Figure 4c. Figure 4, d and e, displays the results for OE and DN PKCη, respectively. Comparing Figure 4e with the control, we find that PKCη DN does not significantly change the Cdc42 zone activity level.

These results are consistent with experimental observations for PKCη DN perturbations.

PKCη OE observations provide additional insights. Vaughan et al. (2014) found that in 80% of observed cells, the Rho zone was completely abolished, whereas the Cdc42 zone persisted, with relatively unchanged brightness. A comparable PKCη OE simulation (Figure 4c), with PKC affecting Cdc42 and Rho equally, mirrors this observation: the Rho zone is abolished, and the Cdc42 zone remains. Although this result depends on parameters of the model (which are chosen for best fit, not measured experimentally), it provides proof of principle that PKCη perturbations can result in asymmetric zone dynamics. These results further support the hypothesis that PKCη acts on a GTPase inactivation rate (or alternatively on a GTPase basal activation rate; similar results, not shown).

To summarize, before modeling, we knew that PKCη and PKCβ have opposing influences on the intensity and persistence of GTPase zones around a single-cell wound. Taken together, our modeling results, in combination with experimental observations, suggest that the PKCs affect distinct targets and that PKCβ is most likely affecting positive feedback strength in the Rho–Abr and Cdc42 activation pathways, whereas PKCη is affecting either inactivation or basal rates of activation of Rho and Cdc42.

Spatial dependence
Thus far, we have simplified the description of PKCβ and PKCη actions as spatially uniform on the region near the wound edge. In fact, both PKCs are distributed nonuniformly next to the wound edge (Vaughan, 2014). Fluorescence quantification of PKCη shows high activity near the wound edge that drops off further away. Here we consider how spatial variation in the PKCη activity

affects our conclusions and, in particular, how such nonuniformity accounts for more complex observations.

Recall that in 80% of PKCη OE experiments, the Rho zone is abolished. In those experiments, the Cdc42 zone persists but, of interest, fails to encroach on the wound edge. That is, the Cdc42 zone remains in the same location, even when the Rho zone fails to form. This is surprising, given the supposition that Rho activity prevents Cdc42 from invading into the region adjacent to the wound by Abr-mediated Cdc42 inactivation (Chuang et al., 1995). On the basis of this, we deduce that some other Cdc42 inhibition maintains that suppression.

We next investigated our revised model predictions when PKCη influences both Rho and Cdc42 inactivation rates. On the bifurcation diagram (Figure 5a), we display both Cdc42 and Rho steady-state activities (vertical axis) as the PKCη effect (acting jointly and symmetrically on d_C and d_R) is varied. We also considered the possibility that rather than being spatially uniform, PKCη activity is graded and decreases away from the wound edge as shown in Figure 5b (this assumption simplifies away the details of the few micrometers adjacent to the wound edge).

We can now reinterpret the bifurcation diagram of Figure 5a in terms of distance from the wound edge. From right to left, the diagram captures conditions at increasing distance (decreasing PKCη) away from the wound edge. From Figure 5a, we see that at high PKCη activity ("close to the wound"), neither zone can form (only the low branch of the diagram, representing background level of
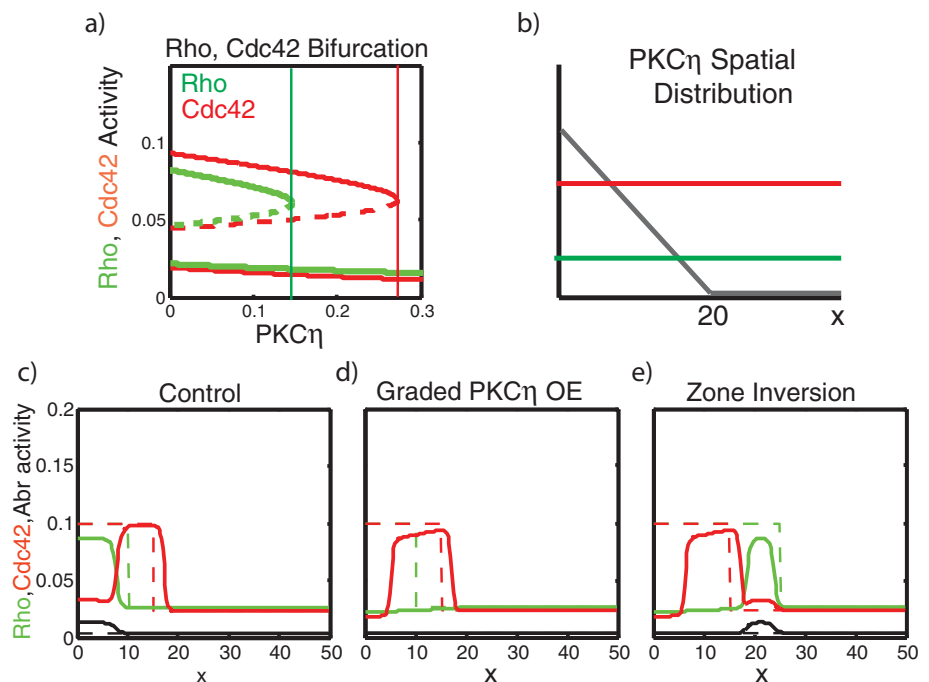

FIGURE 5: Model predictions for graded PKCη activity and predicted zone inversion. (a) Bifurcation plot for the case where PKCη jointly influences Rho and Cdc42. For PKCη activity levels higher than the value indicated by green (respectively red) line, the Rho (respectively Cdc42) zone cannot form due to excessive inactivation (bistability is required for each zone formation and only exists *below* those PKCη activity levels). (b) The assumed PKCη spatial distribution (linearly graded, with value η = 3 at the wound edge and η = 0 at 20 μm away). Red and green lines have the same meaning as in a. (c) Control simulation for comparison. (d) Graded PKCη overexpression ($d\eta_R = d\eta_C = 0.1$) suppresses the Rho zone. The Cdc42 zone persists and stays in the same location. (e) Same as in d, but with an extended Rho initial condition that represents some fraction (20%) of PKCη OE cells. The initial condition for Rho is the same as in previous simulations but is extended to a distance of 20 μm from the wound edge (mimicking a possible extension of the zone of initial Rho activity). Zone inversion occurs.

GTPases, is present). For lower PKCη, only the Cdc42 zone is possible (upper branch of the red, z-shaped curve), whereas Rho is at a low, background level. This forces the Cdc42 zone to stay at its usual location away from the wound. As PKCη level drops to even lower levels ("further away from the wound"), high Rho activity levels are again possible. Summarizing, to the right of the green vertical line, inactivation is strong enough to prevent the Rho zone from being established. Similarly, to the right of the red line, a Cdc42 zone is not possible. Between those two lines, however, the Cdc42 zone can form and persist, whereas the Rho zone cannot.

We repeated model simulations based on this scenario. Control conditions are shown in Figure 5c for comparison. In Figure 5d, we show the result of graded PKCη OE. We see that the Cdc42 zone indeed persists and stays in its usual location, whereas the Rho zone disappears, as our bifurcation analysis suggested. Thus results of this model variant are consistent with experimental observations: the Rho zone is abolished, but the remaining Cdc42 zone does not get closer to the wound edge. Hence we find that the spatially non-uniform activity of PKCη is consistent with both 1) the sole presence of the Cdc42 zone and 2) the location of that zone when the Rho zone does not form.

Zone inversion

The most surprising of the experimental observations is that in 20% of PKCη OE cells, both Rho and Cdc42 zones appear, but with inverted localization. That is, the Cdc42 zone remains in the normal location, but the Rho zone appears on its periphery, away from the wound edge. This is a particularly distinguishing observation, and many simple assumptions on PKC dynamics fail to recapitulate this observation Liao, 2013.

We hypothesize that this is the result of a stochastic effect related to initial Rho activity levels immediately after wounding. Recall that in Simon et al. (2013) and in our model revisions, zones are formed when a positive feedback loop in a bistable system is triggered by superthreshold GTPase level locally driving GTPase activity to its elevated state. Although we have no details concerning the initial trigger, we typically hypothesize initial GTPase levels that exceed the given sensitivity threshold at some locations.

In this hypothesis, a stimulus is required to raise initial GTPase levels beyond the threshold needed to trigger the positive feedback. If initial levels were well below the necessary threshold beyond the Cdc42 zone, no cells would exhibit zone inversion. If that initial level were considerably above the necessary threshold, all cells would exhibit the inversion. Because only a fraction of cells exhibit this inversion, we hypothesize that the initial Rho response generated by the wound is near this threshold and that stochastic effects cause the feedback to be triggered in only some (i.e., 20%) of the cells. In control cells, imaging indicates that Rho levels (before zone formation, that is) are initially elevated near the wound edge. We hypothesize that, in the PKCη OE cells, this region of initial elevation extends further away from the wound edge and is responsible for the initiation of a zone further away.

To test this, we inspected more closely the PKCη OE results (Figure 7c in Vaughan et al., 2014). This reveals that in the 80% of cells that do not exhibit the inversion, elevated levels of Rho activity are found beyond the Cdc42 zone. Although this is not a marked increase, visual inspection does suggest that it is above background. We note again that a dramatic increase in Rho activity levels should not be expected, as that would trigger zone establishment in all cells. Thus the presence of this extended region of elevated Rho activity, along with the rather faint nature of that activity, supports the hypothesis that the inverted Rho zone is a stochastic effect resulting from a near-threshold increase in initial Rho levels.

We tested this idea by simulating the same model with spatial PKCη OE but with initial conditions that included elevated Rho levels throughout the domain. As shown in Figure 5e, this model generates inverted zones: the Rho zone is now on the outside of the Cdc42 zone, which stays in its usual location, as before. Hence we confirm that if the Rho activity is initially elevated in a subset of PKCη OE cases, it can lead to the zone inversion in that subset of cells. At this point, we cannot speculate what the source of this extended zone of initially elevated Rho activity is in PKCη OE conditions.

DISCUSSION

Single-cell repair offers a powerful model for understanding subcellular patterning by Rho GTPases. The power arises from the simplicity of the signal and the speed and predictability of the response: calcium entering the cell through the hole in the plasma membrane triggers activation of the Rho GTPases, which then sort into complementary zones around the wound, all within 60–120 s, depending on the model (Benink and Bement, 2005; Abreu-Blanco et al., 2014). However, even in this narrow time window, there is a surprising degree of complexity. In the Xenopus system, for example, formation of the GTPase zones results from (at a minimum) a combination of positive feedback within zones and negative cross-talk between zones (Simon et al., 2013; Vaughan et al., 2014) and rapid, local GTPase inactivation (Burkel et al., 2012).

The foregoing events and processes, although complex, are still within the grasp of intuition. However, efforts to identify the steps that link the calcium inrush to GTPase zone formation added new players and mechanisms that defy straightforward explanations (Vaughan et al., 2014). In particular, two findings seem especially peculiar. First, protein kinases Cβ and η have partially overlapping distributions around wounds but apparently have antagonistic functions—PKCβ stimulates the GTPases, whereas PKCη inhibits them. Second, overexpression of PKCη produces a mix of phenotypes: ~80% of the cells display a sharp reduction of Rho activity around wounds, and the remaining ~20% display zone inversion, with the Rho zone becoming displaced outside the Cdc42 zone (Vaughan, 2014).

The modeling approach used here has allowed us to overcome the limits of intuition. On the basis of our results, we propose the following specific roles for PKCβ and PKCη. PKCβ is most likely to function by increasing the positive feedback that underlies the rapid amplification of Rho and the Cdc42 during zone formation. In the case of Rho, this feedback results from Abr-mediated Rho activation and Rho-mediated recruitment of Abr (Vaughan et al., 2011; Simon et al., 2013). Thus Abr is a reasonable candidate for PKC-dependent Rho phosphorylation, although we know of no evidence that Abr is indeed subject to regulation by phosphorylation. The basis of the positive feedback that promotes explosive Cdc42 activation during zone formation is unknown, so we cannot speculate on a specific PKCβ target at this point. It also remains possible that the same PKCβ substrate is responsible for up-regulation of both feedback loops. RhoGDI, for example, is a known target of conventional protein kinases C (of which PKCβ is an example; Dovas, 2010) and a binding partner for both Rho and Cdc42 (Dovas and Couchman, 2005). Given that RhoGDI is believed to limit access of RhoGTPases to GEFs, if phosphorylation suppresses RhoGDI's ability to bind the GTPases, this might be expected to promote positive feedback.

Regardless of the relevant PKCβ target(s), these findings suggest that PKCβ is responsible for establishing the "playing field" for

GTPase signaling. That is, the GTPase zones are normally confined to a circular region that extends ~5–10 μm away from the wound. Because PKCβ is recruited to this same general area before the zones arise, we suggest that it defines the region of the plasma membrane that is competent to support zone activity.

PKCη is most likely to function by increasing the inactivation rate of Rho and Cdc42 or by reducing the basal rates of GTPase activation. Rho GTPase inactivation is the province of GAPs, and thus PKCη might function by elevating GAP activity, although we are not aware of examples of GAP PKCη substrates. It is also conceivable that RhoGDIs might again be the target, assuming that phosphorylation by PKCη increases their affinity for Rho and Cdc42.

With respect to general function, we suggest that PKCη plays two roles: first, it helps limit Rho activity both by competing with PKCβ for DAG binding and by increasing the inactivation rate of Rho. Second, it provides a second means (in addition to the GAP activity of Abr) for keeping the Cdc42 zone distal to the wound edge.

In summary, the modeling results presented here provide testable explanations for the previously counterintuitive findings concerning PKC-mediated control of Rho GTPase activity in cell repair. They also provide an intellectual framework for understanding the higher-order regulation of GTPase activation and cross-talk. We look forward to identification of the key targets of the protein kinases C in this process as a means to test some of the ideas generated here.

REFERENCES
Abreu-Blanco MT, Verboon JM, Parkhurst SM (2014). Coordination of Rho family GTPase activities to orchestrate cytoskeleton responses during cell wound repair. Curr Biol 24, 144–155.

Amano M, Fukata Y, Kaibuchi K (2000). Regulation and functions of Rho-associated kinase. Exp Cell Res 261, 44–51.

Bement WM, Miller AL, von Dassow G (2006). Rho GTPase activity zones and transient contractile arrays. BioEssays 28, 983–993.

Benink HA, Bement WM (2005). Concentric zones of active RhoA and Cdc42 around single cell wounds. J Cell Biol 168, 429–439.

Bishop AL, Hall A (2000). Rho GTPases and their effector proteins. Biochem J 348, 241–255.

Burkel BM, Benink HA, Vaughan EM, von Dassow G, Bement WM (2012). A Rho GTPase signal treadmill backs a contractile array. Dev Cell 23, 384–396.

Chuang TH, Xu X, Kaartinen V, Heisterkamp N, Groffen J, Bokoch GM (1995). Abr and Bcr are multifunctional regulators of the Rho GTP-binding protein family. Proc Natl Acad Sci USA 92, 10282–10286.

Clark AG, Miller AL, Vaughan E, Yu HY, Penkert R, Bement WM (2009). Integration of single and multicellular wound responses. Curr Biol 19, 1389–1395.

Dovas A, Choi Y, Yoneda A, Multhaupt HA, Kwon SH, Kang D, Oh ES, Couchman JR (2010). Serine 34 phosphorylation of rho guanine dissociation inhibitor (RhoGDIalpha) links signaling from conventional protein kinase C to RhoGTPase in cell adhesion. J Biol Chem 285, 23296–23308.

Dovas A, Couchman JR (2005). RhoGDI: multiple functions in the regulation of Rho family GTPase activities. Biochem J 390, 1–9.

Edelstein-Keshet L, Holmes WR, Zajac M, Dutot M (2013). From simple to detailed models for cell polarization. Philos Trans R Soc Lond B Biol Sci 368, 20130003.

Ferrell JE, Xiong W (2001). Bistability in cell signaling: how to make continuous processes discontinuous, and reversible processes irreversible. Chaos 11, 227–236.

Holmes WR (2014). An efficient, nonlinear stability analysis for detecting pattern formation in reaction diffusion systems. Bull Math Biol 76, 157–183.

Holmes WR, Lin B, Levchenko A, Edelstein-Keshet L (2012). Modelling cell polarization driven by synthetic spatially graded rac activation. PLoS Comput Biol 8, e1002366.

Holmes WR, Mata MA, Edelstein-Keshet L (2015). Local perturbation analysis: a computational tool for biophysical reaction-diffusion models. Biophys J 108, 230–236.

Jilkine A, Maree AFM, Edelstein-Keshet L (2007). Mathematical model for spatial segregation of the Rho-family GTPases based on inhibitory cross-talk. Bull Math Biol 69, 1943–1978.

Kono K, Saeki Y, Yoshida S, Tanaka K, Pellman D (2012). Proteasomal degradation resolves competition between cell polarization and cellular wound healing. Cell 150, 151–164.

Liao L (2013). Signalling in Single Cell Wound Healing. MSc Thesis. Vancouver, BC, Canada: Department of Mathematics, University of British Columbia. Available at https://circle.ubc.ca/handle/2429/44784 (accessed 1 July 2015).

Lin B, Holmes WR, Wang CJ, Ueno T, Harwell A, Edelstein-Keshet L, Inoue T, Levchenko A (2012). Synthetic spatially graded Rac activation drives cell polarization and movement. Proc Natl Acad Sci USA 109, E3668–E3677.

Mandato CA, Bement WM (2001). Contraction and polymerization cooperate to assemble and close actomyosin rings around Xenopus oocyte wounds. J Cell Biol 154, 785–797.

Maree AFM, Jilkine A, Dawes A, Grieneisen VA, Edelstein-Keshet L (2006). Polarization and movement of keratocytes: a multiscale modelling approach. Bull Math Biol 68, 1169–1211.

Moon SY, Zheng Y (2003). Rho GTPase-activating proteins in cell regulation. Trends Cell Biol 13, 13–22.

Mori Y, Jilkine A, Edelstein-Keshet L (2011). Asymptotic and bifurcation analysis of wave-pinning in a reaction-diffusion model for cell polarization. SIAM J Appl Math 71, 1401–1427.

Nobes CD, Hall A (1995). Rho, rac and cdc42 GTPases: regulators of actin structures, cell adhesion and motility. Biochem Soc Trans 23, 456–459.

Olofsson B (1999). Rho guanine dissociation inhibitors: pivotal molecules in cellular signalling. Cell Signal 11, 545–554.

Rossman KL, Der CJ, Sondek J (2005). GEF means go: turning on Rho GTPases with guanine nucleotide-exchange factors. Nat Rev Mol Cell Biol 6, 167–180.

Simon CM, Vaughan EM, Bement WM, Edelstein-Keshet L (2013). Pattern formation of Rho GTPases in single cell wound healing. Mol Biol Cell 24, 421–432.

Sonnemann KJ, Bement WM (2011). Wound repair: toward understanding and integration of single-cell and multicellular wound responses. Annu Rev Cell Dev Biol 27, 237–263.

Tyson JJ, Chen KC, Novak B (2003). Sniffers, buzzers, toggles and blinkers: dynamics of regulatory and signaling pathways in the cell. Curr Opin Cell Biol 15, 221–231.

Vaughan EM, Miller AL, Yu HYE, Bement WM (2011). Control of local Rho GTPase crosstalk by Abr. Curr Biol 21, 270–277.

Vaughan EM, You JS, Elsie Yu HY, Lasek A, Vitale N, Hornberger TA, Bement WM (2014). Lipid domain-dependent regulation of single-cell wound repair. Mol Biol Cell 25, 1867–1876.